

# Identification of a Blue Copper Protein from *Hyphomicrobium denitrificans* and its Functions in the Periplasm

Daisuke Hira, Masaki Nojiri, Kazuya Yamaguchi and Shinnichiro Suzuki\*

Department of Chemistry, Graduate School of Science, Osaka University, 1-16 Machikaneyama, Toyonaka, Osaka 560-0043, Japan

Received April 9, 2007; accepted June 13, 2007; published online July 23, 2007

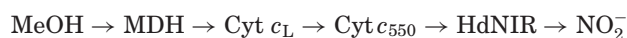
It has been known that the methylotrophic denitrifying bacteria have the specific electron transfer chains, involving in 'methanol oxidation' and 'denitrification', in the periplasm. Recently, a unique blue copper protein (HdBCP) has been isolated from the methanol-grown methylotrophic denitrifying bacterium, *Hyphomicrobium denitrificans*. HdBCP is a 14.5 kDa protein and contains one copper atom in the molecule. The electronic absorption spectrum of HdBCP exhibits two absorption maxima near 450 and 750 nm comparable with the intense 600 nm band ( $\epsilon_{450}/\epsilon_{600} = \text{ca. } 0.9$ ). The rhombic electron paramagnetic resonance spectrum shows clearly that the copper centre is a 'perturbed' type 1 copper geometry. Stopped-flow kinetics indicates that HdBCP accepts efficiently an electron from cytochrome  $c_L$  ( $k_2 = 4.0 \times 10^6 \text{ M}^{-1} \text{ s}^{-1}$  at 25.0°C), which is a physiological electron acceptor for methanol dehydrogenase. According to cloning and DNA sequencing of the structural gene, the deduced amino acid sequence shows significant similarities with pseudoazurins, which are a physiological electron donor for Cu-containing nitrite reductase from the denitrifying bacteria. Based on these results, we discuss the role of HdBCP in the electron-flow system, which link 'methanol oxidation' and 'denitrification' together.

**Key words:** blue copper protein, denitrification, electron transfer, methylotroph, type 1 copper.

Abbreviations: BCP, blue copper protein; NIR, nitrite reductase; HdNIR, Cu-containing nitrite reductase from *Hyphomicrobium denitrificans*; MDH, methanol dehydrogenase; Cyt  $c_L$ , cytochrome  $c_L$ ; Cyt  $c_{550}$ , cytochrome  $c_{550}$ ; Am, amicyanin; Az, azurin; PAz, pseudoazurin; Hd, *Hyphomicrobium denitrificans*; Af, *Alcaligenes faecalis*; Ac, *Achromobacter cycloclastes*; Ax, *Alcaligenes xylosoxidans*; Pp, *Paracoccus pantotrophus*; Me, *Methylobacterium extorquens* AM1; EPR, electron paramagnetic resonance; ET, electron transfer.

*Hyphomicrobium denitrificans* is a methylotrophic denitrifying bacterium, capable of growth with methanol as a sole carbon source (1, 2). Methanol is oxidized to formaldehyde by the reduction of pyrroloquinoline quinone (PQQ) in methanol dehydrogenase (MDH), and then the reduced PQQ transfers electrons to a physiological electron acceptor cytochrome  $c_L$  (Cyt  $c_L$ ) (3–8). Cyt  $c_L$  is subsequently oxidized by cytochrome  $c_{550}$  [Cyt  $c_{550}$  corresponds to cytochrome  $c_H$  from methylotrophic bacteria (7, 9–11)]. Moreover, copper-containing nitrite reductase (NIR) and nitrous oxide reductase ( $\text{N}_2\text{OR}$ ) involving in denitrification have been also purified from Hd cells grown on methanol (12–14). Recently, X-ray crystal structure of novel hexameric HdNIR has been determined (15). The molecular structure reveals a trigonal-prism-shaped homohexamer (a tightly associated dimer of trimers), in which the monomer consisting of 447 residues and three Cu atoms are organized. NIR is a key enzyme in denitrification, catalyzing the first step that leads to gaseous products ( $\text{NO}_2^- + e^- + 2\text{H}^+ \rightarrow \text{NO} + \text{H}_2\text{O}$ ). The efficient electron

donation from the specific electron donor protein to the enzyme is necessary for the catalytic cycle. In the case of Hd, the electron donor protein is Cyt  $c_{550}$  (13, 15), which is a physiological electron acceptor for Cyt  $c_L$ . Therefore, the electron derived from methanol flows to HdNIR constituting the nitrate respiration system in the periplasmic space of a methylotrophic denitrifying bacterium, Hd as follows:



In general, three bacterial blue copper proteins (BCPs), amicyanins (Am) (16–23), azurins (Az) (24–29) and pseudoazurins (PAz) (16, 17, 30, 31), have been found in several methylotrophic or denitrifying bacteria. These are small electron transfer (ET) proteins characterized by an intense electronic absorption band near 600 nm (blue band) and a small hyperfine coupling constant (5–7 mT) in EPR spectra, which originate in the type 1 copper. The visible absorption spectra of Az and Am reveal a weak 450 nm band compared with the blue band ( $\epsilon_{450}/\epsilon_{\text{blue}} = 0.1–0.2$ ) (16, 18, 20, 26), while that of PAz exhibits two clear absorption maxima near 450 and 750 nm, compared with the most intense blue band ( $\epsilon_{450}/\epsilon_{\text{blue}} = 0.4–0.5$ ) (16, 31). The EPR signals of Az and Am show axial symmetries, but that of PAz indicates a rhombic symmetry.

\*To whom correspondence should be addressed. Tel: +81-6-6850-5767, Fax: +81-6-6850-5785, E-mail: bic@ch.wani.osaka-u.ac.jp

Blue Am is located in the periplasm of methylotrophic bacteria such as *Paracoccus denitrificans* (20, 23) and *Methylobacterium extorquens* AM1 (Me) (16–18), being the smallest BCP having 99–105 amino acid residues. Its principal function is to accept electrons from methylamine dehydrogenase (MADH, EC 1.4.99.3) containing tryptophan tryptophylquinone (TTQ) and to transfer them to one or more cytochromes. On the other hand, two Az's (Az-iso1 and Az-iso2) have been identified from the obligate methylotroph *Methylomonas* sp. strain J isolated from garden soil by selection on a medium containing methylamine as the sole carbon source (24, 25). Both Az's are expressed when the cells are grown on methylamine, but only Az-iso1 is detected when methanol is used instead of methylamine. Recently, it has been demonstrated that Az-iso2 is a direct electron acceptor for MADH *in vivo* (32).

In denitrification, greenish-blue PAz is obviously an electron donor for green Cu-containing NIRs (33–36). The former is a basic protein, and the latter is acidic. The second-order rate constant ( $k_{ET}$ ) of intermolecular ET from *Achromobacter cycloclastes* (Ac) PAz to its cognate NIR was estimated to be  $7.3 \times 10^5 \text{ M}^{-1} \text{ s}^{-1}$  (pH 7.0) by cyclic voltammetry (33). The electrostatic interaction between the basic amino acid residues of the PAz from *Alcaligenes faecalis* (Af) S-6 and the acidic amino acid residues of its cognate NIR is proposed by X-ray crystal structure analyses and kinetics (35). Moreover, blue Az is also expressed in some denitrifying bacteria under anaerobic growth. It has been suggested that both Az and cytochrome  $c_{551}$  (Cyt  $c_{551}$ ) receive electrons from  $bc_1$  complex and donate them to NIR (37). Az was also reported as an electron donor for the Cu-containing NIRs from *Pseudomonas aureofaciens* (38) and *Alcaligenes xylooxidans* (Ax) NCIMB 11015 (27). However, the cyclic voltammeteries of the Az-I and Az-II from Ax exhibited little response in the presence of the enzyme and nitrite, indicating the very slow ET processes ( $k_{ET} < 10^4 \text{ M}^{-1} \text{ s}^{-1}$ ) (36). An *in vivo* approach with *P. aeruginosa* mutants deficient in one or both Cyt  $c_{551}$  and Az have shown that an electron donor for heme  $cd_1$ -containing NIR is Cyt  $c_{551}$ , and not Az (39).

Recently, we have found a unique BCP in the periplasmic fraction of Hd cells grown on methanol. The protein was rapidly reduced with a physiological electron acceptor for MDH, Cyt  $c_L$ , under the physiological conditions. The spectroscopic characterization and the stopped-flow kinetic measurements of the ET between the protein and Cyt  $c_L$  were performed. Furthermore, the structure gene was cloned and the deduced amino acid sequence was analysed.

## MATERIALS AND METHODS

**Preparation of the Blue Copper Protein from *H. denitrificans***—For isolation of Hd blue copper protein (HdBCP), Hd A3151 was cultured as previously described (1). The cells suspended in 40 mM Tris-HCl buffer (pH 7.5) containing 0.5 mM phenylmethanesulfonyl fluoride were sonicated at 180 W for 30 min. The resulting cell debris was removed by centrifugation at 15,000 rpm for 1 h at 4°C. After centrifugation,

the supernatant was applied directly onto a Super Q-Toyopearl column (5 × 15 cm, Tosoh) pre-equilibrated with 40 mM Tris-HCl buffer (pH 7.5). The column was washed with the four volumes of the same buffer, and HdBCP was not adsorbed to the column. The flow-through fraction was further applied onto a Q-Sepharose Fast Flow column (2.5 × 25 cm, Amersham). HdBCP was passed through the column again. Ammonium sulphate was added to a final concentration of 60% saturation to the resulting flow-through fraction (approximately 11). The resulting precipitate was removed by centrifugation (8,000 rpm for 40 min at 4°C). The supernatant was applied onto a Phenyl-Sepharose Fast Flow column (2.5 × 25 cm, Amersham) pre-equilibrated with 40 mM Tris-HCl (pH 7.5) containing a 60% saturated concentration of ammonium sulphate. HdBCP adsorbed on the column was eluted with a linear gradient from 60 to 0% saturated concentration of ammonium sulphate in the same buffer. The HdBCP-containing fractions were collected and then dialyzed with 10 mM potassium phosphate (pH 6.0) for 12 h. The dialyzed sample was applied onto a CM-Sepharose Fast Flow column (2.5 × 25 cm, Amersham) pre-equilibrated with 10 mM potassium phosphate buffer (pH 6.0). HdBCP was eluted with a linear gradient from 10 to 200 mM potassium phosphate (pH 6.0). The collected HdBCP fractions were dialyzed with 10 mM potassium phosphate buffer (pH 6.0) and then applied onto a Resource S column (1.6 × 3.0 cm, Amersham). HdBCP was eluted with a linear gradient from 10 to 80 mM potassium phosphate buffer (pH 6.0). The fractions were collected, concentrated and desalted with a Centriprep-YM10 (Millipore). The purity was estimated to be 90% over by SDS-PAGE. The yield was ca. 1.0 mg/60 g of wet cells.

**Physical Measurements**—The electronic absorption and CD spectra were measured at 25°C with a Shimadzu UV-2450 spectrophotometer and a J-500A spectropolarimeter (JASCO), respectively. The EPR spectrum was recorded with a JEOL JES-FE1X X-band spectrometer at 77 K. The copper content was determined with a Nippon Jarrel Ash AA-880 Mark-II atomic absorption spectrophotometer. Cyclic voltammetric analysis was carried out using a Bio analytical Systems Model CV-50W voltammetric analyser with a three-electrode system consisting of a Ag/AgCl reference electrode, a gold wire counter electrode, and a bis(4-pyridyl)disulfide-modified gold working electrode under Ar atmosphere.

**Stopped-Flow Kinetics**—Stopped-flow experiments were carried out at 25.0°C with a RA-2000 stopped-flow spectrophotometer (Otsuka Electronics). The rapid oxidation of reduced Cyt  $c_L$  with HdBCP was monitored at 417 nm, which is the wavelength of the maximum peak ( $\Delta\varepsilon = 57.2 \text{ mM}^{-1} \text{ cm}^{-1}$ ) in the difference absorption spectrum between the ferrous and ferric forms of Cyt  $c_L$ . The extinction coefficient of HdBCP is  $1.7 \text{ mM}^{-1} \text{ cm}^{-1}$  at 417 nm. To determine the kinetic constants, the concentrations of HdBCP were up to 10-fold greater than that of Cyt  $c_L$ . Pseudo-first-order rate constants were calculated by non-linear regression with a IgorPro version 5.0 (WaveMetrics). The data obtained were the average of at least three experiments (the errors were normally within 5%).

**N-terminal Amino Acid Sequencing of Mature HdBCP and Five Tryptic-Digested Peptides**—The purified HdBCP (200  $\mu$ g) was digested with TPCK-treated trypsin (2  $\mu$ g) at 30°C for 3 h in 100 mM Tris-HCl (pH 8.0) containing 2 M Urea. The five tryptic-digested peptides were separated with a YMC-Pack ODS-A302 reverse-phase column using a 0.1% (v/v) trifluoroacetic acid solution and a 95% acetonitrile solution containing 0.1% trifluoroacetic acid. HPLC was carried out at a flow rate of 0.25 ml/min by continuous monitoring of the 215 nm absorbance. The N-terminal amino acids of the purified mature HdBCP and the five peptide fragments were determined using a Model 477A protein sequencer (ABI).

**Cloning of the Structural Gene of HdBCP**—The N-terminal amino acid sequence of mature HdBCP was A-E-H-I-V-E-M-R-N-K-D-D-A-G-N-T-M-V-F-Q showing a significant similarity (ca. 50%) with that of *P. pantotrophus* PAz. One of the five peptides was K-R-L-D-G-E-I-A, showing a significant similarity with the C-terminal sequence of PAz. PCR with the Hd genomic DNA as a template was performed using two primers (5'-cacatagtg gagatgcgcaacaaggacgac-3' and 5'-ggcgatctcgccgtc cagccgctt-3') designed manually from both N- and C-terminal amino acid sequences and from DNA homology analysis in all PAz's nucleotide sequences. The resulting ca. 360-bp DNA fragment was amplified. The fragment was inserted into the pTA2 vector (Toyobo). The resulting plasmid, pTABCP was digested with *Eco*RI. The ca. 360-bp DNA fragment was inserted into the *Eco*RI site of plasmid pUC119. The full length of the insert DNA was sequenced. Since the sequence analysis clearly showed that the insert DNA is a partial structural gene for HdBCP, the fragment DNA was used as a specific probe for the next colony hybridization step. The *Eco*RI-digested Hd genome DNA fragments (size fraction 2 to 4 kbp) were ligated with Charomid 9-36 DNA (Nippon Gene) linearized with *Eco*RI. The mixture was used directly for *in vitro* packaging using *In vitro* Packaging Kit LAMBDA INN (Nippon Gene) with *Escherichia coli* DH5a as a host. Colony hybridization was carried out by use of AlkPhos Direct labelling Hybridization kit (GE Healthcare) for the total 2,000 colonies obtained.

## RESULTS AND DISCUSSION

**Purification of *H. denitrificans* Blue Copper Protein (HdBCP)**—The two cytochromes *c* (Cyt *c*<sub>L</sub> and Cyt *c*<sub>550</sub>) are contained in methanol-grown Hd A3151 (8). At the final purification step, both HdBCP and Cyt *c*<sub>550</sub> are adsorbed to a cation-exchange Resource S column at pH 6.0 (10 mM potassium phosphate buffer), and then HdBCP is eluted following weak basic Cyt *c*<sub>550</sub> with a linear gradient from 10 to 80 mM potassium phosphate buffer (pH 6.0) (Fig. 1). The yield of HdBCP was ca. 1.0 mg/60 g of wet cell even if in a methylamine-containing medium (instead of methanol). Interestingly, the yield was dramatically increased, when the ratio of Cu to Fe in the medium was increased (e.g. Cu, 130  $\mu$ M and Fe, 0.35  $\mu$ M). The yield of HdBCP from the cells grown on the modified medium composition was about 30 mg/60 g wet cell. The purified HdBCP gives a single

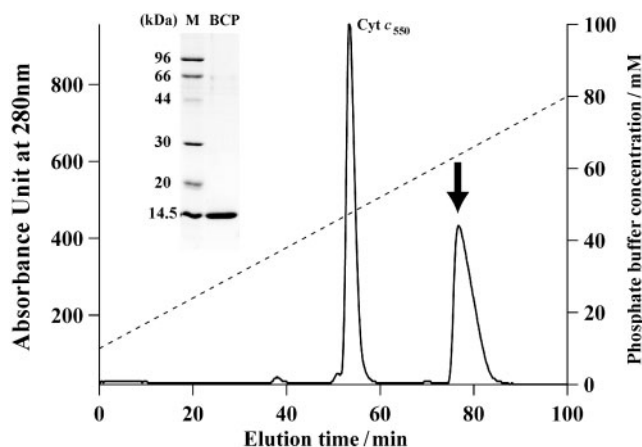


Fig. 1. The Resource S column chromatograph for the purification of HdBCP. Arrow indicates the elution band of HdBCP. The broken line means a linear gradient from 10 to 80 mM potassium phosphate buffer (pH 6.0). Inset, SDS-PAGE of purified HdBCP (2 mg). M is a molecular weight marker set.

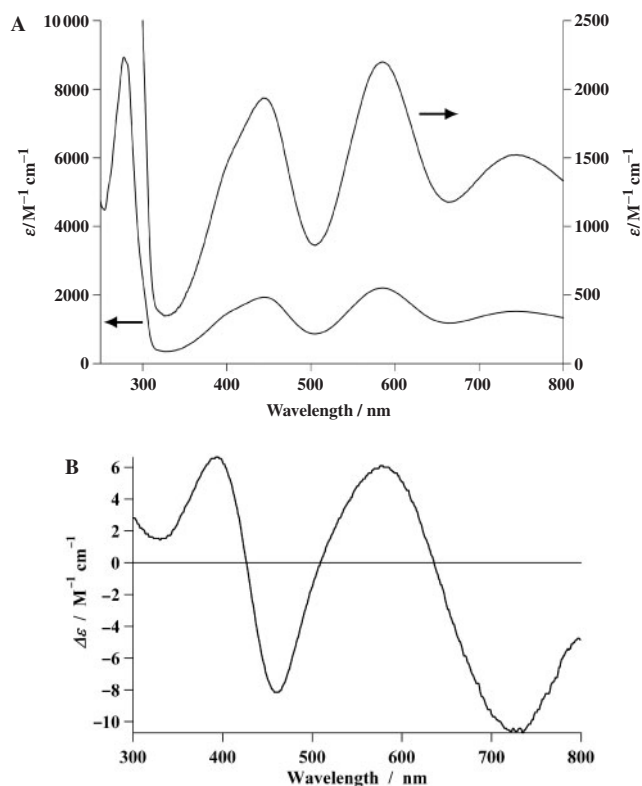


Fig. 2. Electronic absorption (A) and CD (B) spectra of HdBCP in 10 mM potassium phosphate buffer (pH 6.0) at room temperature.

band at a molecular mass of 14.5 kDa on the SDS-PAGE (Fig. 1, inset). The copper content was determined to be 0.95/mol of the protein by an atomic absorption spectroscopy.

**Spectroscopic Characterization of HdBCP**—Figure 2 shows the electronic absorption (A) and CD (B) spectra of HdBCP in 10 mM phosphate buffer at pH 6.0.

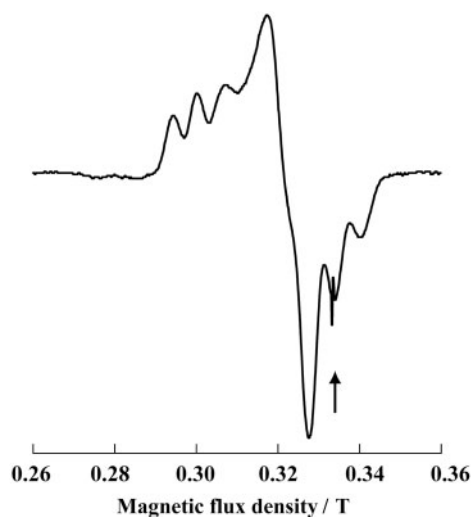


Fig. 3. EPR spectrum of HdBCP in 10 mM potassium phosphate buffer (pH 6.0) at 77 K. Allow indicates an internal standard signal (TCNQ).

The visible absorption spectrum exhibits three peaks at 444 ( $\epsilon=1,940$ ), 585 ( $\epsilon=2,200$ ) and 745 nm ( $\epsilon=1,520 \text{ M}^{-1} \text{ cm}^{-1}$ ). The intense ca. 600 nm band and the spectral pattern of HdBCP are quite similar to those of cucumber basic protein (CBP) from plant (40–42) rather than those of the well-known BCPs (Am, Az and PAz) from the methylotrophic or denitrifying bacteria. The visible CD spectrum shows four extrema at 394 ( $\Delta\epsilon=6.64$ ), 460 ( $\Delta\epsilon=-8.14$ ), 578 ( $\Delta\epsilon=6.09$ ) and 728 nm ( $\Delta\epsilon=-10.6 \text{ M}^{-1} \text{ cm}^{-1}$ ), and zero-crossings occur at 427, 509 and 636 nm. Therefore, the characteristic intense electronic absorption band around 450 nm is caused by intense positive and negative CD transitions at 394 and 460 nm, respectively. The ca. 450 nm electronic absorption band most likely consists of (His)N $\delta$ 1  $\rightarrow$  Cu(II), (Met)S $\delta$   $\rightarrow$  Cu(II) and (Cys)S $\gamma$  (pseudo- $\sigma$ )  $\rightarrow$  Cu(II) charge-transfer transitions (40, 42, 43). The 77-K EPR spectrum of HdBCP in Fig. 3 exhibits a typical rhombic character ( $g_z=2.21$ ,  $g_y=2.08$ ,  $g_x=2.02$ ,  $A_z=6.0 \text{ mT}$  and  $A_x=6.8 \text{ mT}$ ) and shows significant similarities to those of PAz [ $g_z=2.24$ ,  $g_y=2.09$ ,  $g_x=2.02$ ,  $A_z=5.5 \text{ mT}$  and  $A_x=6.8 \text{ mT}$  (44)] and CBP [ $g_z=2.22$ ,  $g_y=2.07$ ,  $g_x=2.02$ ,  $A_z=6.0 \text{ mT}$  and  $A_x=6.0 \text{ mT}$  (40)]. These spectral features are often observed in ‘perturbed’ BCPs, which exhibit substantially different spectral profiles from those of plastocyanin and Am having the ‘classic’ blue copper site (42). Therefore, HdBCP probably has a copper ligand set (Cys, 2His and Met) with shorter axial Cu–S (Met) and longer equatorial Cu–S (Cys) bonds than those of the ‘classic’ blue copper site, which is characterized as a ‘perturbed’ type 1 copper (45–47).

**Intermolecular Electron Transfer Between HdBCP and Cyt  $c_L$** —The cyclic voltammogram of HdBCP shows a midpoint potential ( $E_{1/2}$ ) of +277 mV versus NHE at pH 6.0. To observe the electron-accepting ability of HdBCP, the reduction of HdBCP was monitored spectroscopically in the presence of one or both MDH and Cyt  $c_L$  (Fig. 4A). At first the oxidized HdBCP was mixed with MDH. The visible spectrum was not so changed.

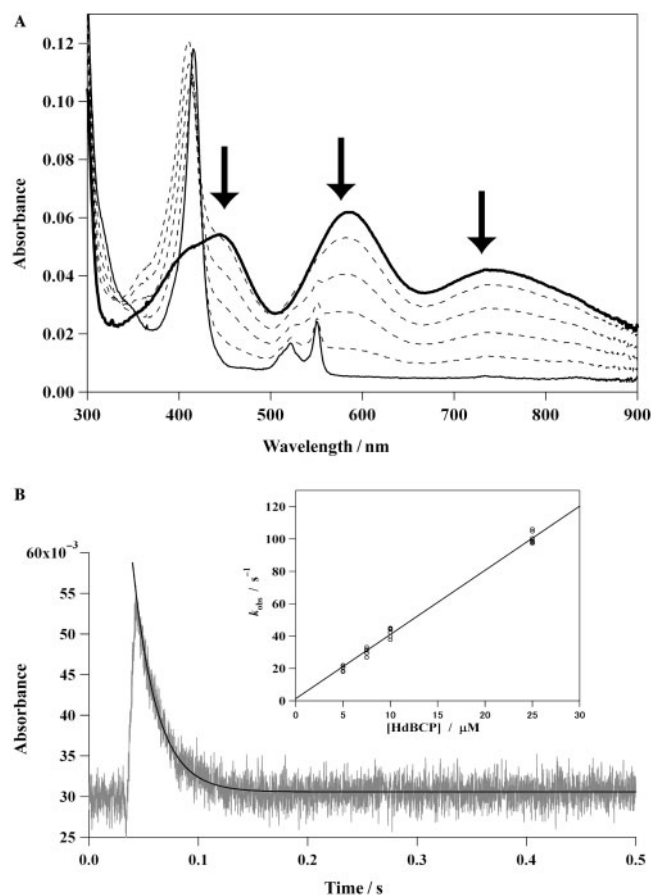


Fig. 4. Intermolecular ET reaction between HdBCP and Cyt  $c_L$ . (A) Bleaching of the visible absorption spectrum of HdBCP with Cyt  $c_L$  and MDH. Thick solid line: the visible absorption spectrum of the mixture of 25  $\mu\text{M}$  HdBCP and 1  $\mu\text{M}$  MDH in 10 mM potassium phosphate buffer (pH 6.0) containing 400 mM methanol. Broken line: the spectra with the 1 min interval, after 1  $\mu\text{M}$  of Cyt  $c_L$  was added to the mixture. Thin solid line: after 5 min. (B) The rapid decay curve observed using stopped-flow spectrophotometer. Ten micromolar HdBCP and 0.5  $\mu\text{M}$  Cyt  $c_L$  were contained in 10 mM potassium phosphate buffer (pH 6.0) containing 200 mM NaCl. Inset: The plot of  $k_{\text{obs}}$  versus HdBCP concentration.

However, further addition of Cyt  $c_L$  to the mixture results in rapid bleaching of the blue band of HdBCP. The findings clearly indicate that HdBCP cannot accept electrons directly from MDH without Cyt  $c_L$ . The detailed kinetics of intermolecular ET between HdBCP and Cyt  $c_L$  has been investigated by a stopped-flow absorption spectrophotometer (Fig. 4B). The  $k_{\text{obs}}$  values were obtained under the conditions that the reaction mixture contains 0.5  $\mu\text{M}$  Cyt  $c_L$  and 5–25  $\mu\text{M}$  HdBCP in the presence of 200 mM NaCl at pH 6.0. The rapid oxidation of Cyt  $c_L$  is monophasic and obeys pseudo-first-order kinetics. From the slope of the plot of  $k_{\text{obs}}$  versus HdBCP concentration, the second-order rate constant ( $k_2$ ) was determined to be  $4.0 (\pm 0.1) \times 10^6 \text{ M}^{-1} \text{ s}^{-1}$  at 25.0°C. Interestingly, the rate constant was similar to that of the intermolecular ET between Cyt  $c_L$  and Cyt  $c_{550}$  [ $6.0 (\pm 0.5) \times 10^7 \text{ M}^{-1} \text{ s}^{-1}$  at 25.0°C, manuscript in preparation; Nojiri, M. *et al.* (8)].

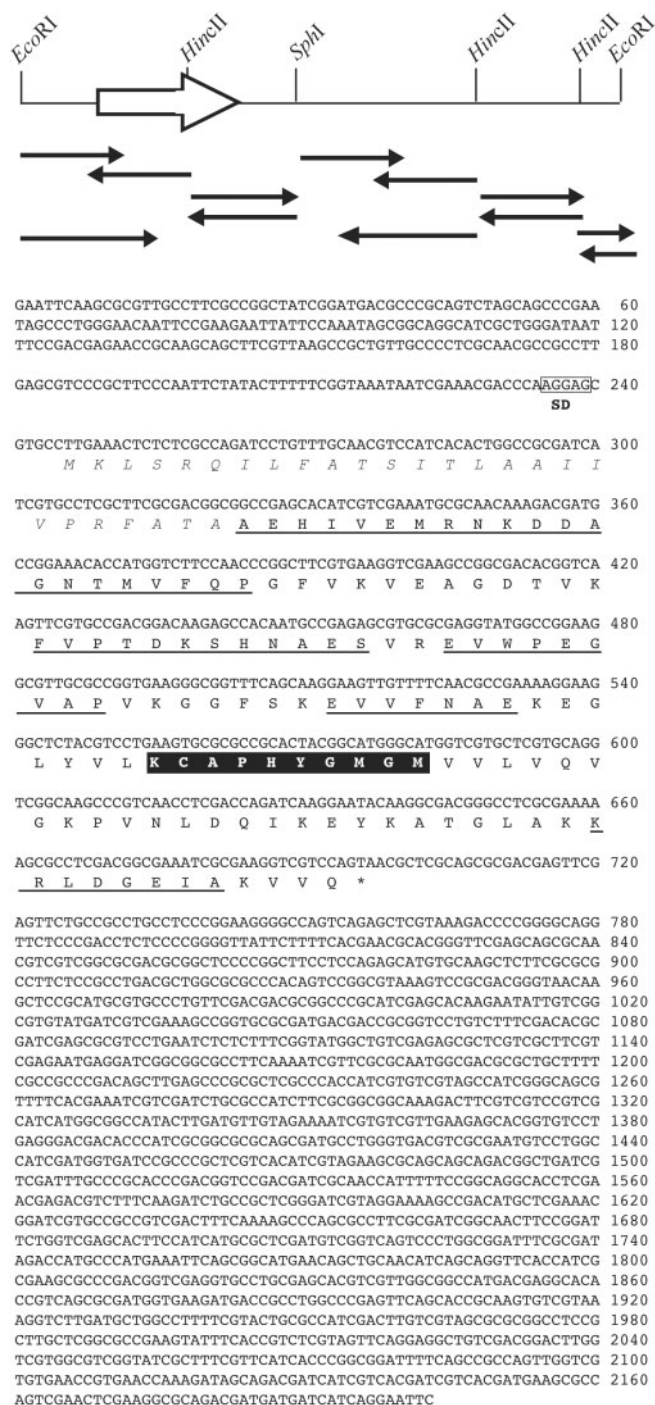


Fig. 5. Nucleotide and deduced amino acid sequence of HdBCP. Upper: schematic figure of the 2.2 kbp *EcoRI* fragment. Thick white allow represents the HdBCP coding region. Black allows represent the sequencing strategies. Lower: nucleotide and deduced amino acid sequence of HdBCP. The deduced amino acid sequence is shown below as a single-letter code. A potential ribosome-binding site (SD) is shown with a box. The analysed N-terminal amino acid sequences are shown with the thin underlines. The deduced signal peptide region is shown in italic. The specific motif [K]-[C]-[T/A]-[P]-[H]-x-[G/A/M]-[M]-[G/S]-[M] for PAz (48) is shown in white on a black background. Nucleotide sequence data reported are available in the DDBJ/EMBL/GenBank databases under accession number AB297894.

**Cloning of the HdBCP Structural Gene and the Deduced Amino Acid Sequence**—To obtain the amino acid sequence information on HdBCP, cloning of the structural gene was performed (MATERIAL AND METHODS). Using the PCR amplified ca. 360 bp DNA fragment as a specific probe, the HdBCP structural gene was screened from a partial genomic library of DNA fragments (ca. 2.0–4.0 kbp) obtained by digestion with *EcoRI*. One positive clone containing ca. 2.2 kbp insert DNA was obtained from colony hybridization and the full length of the fragment was sequenced. BLAST database searching shows obviously that there is one complete open reading frame (ORF) in the fragment (Fig. 5). The deduced amino acid sequence from the nucleotide sequence located at 323 bp downstream region of the *EcoRI* site completely corresponds with the N-terminal amino acid sequence of mature HdBCP, A-E-H-I-V-E-M-R-N-K-D-D-A-G-N-T-M-V-F-Q-. One rare initial TTG codon was found in the upstream region of the GCC codon of the N-terminal Ala. The ribosome-binding site (AGGAG) located at 6 bp upstream region of the TTG codon suggests that the ORF of the HdBCP structural gene includes 452 bp encoding 151 amino acid residues. Ala27 is the N-terminus of mature HdBCP (calculated Mr=13,570) and is preceded by the signal peptide composed of 26 amino acid residues. All of the partial amino acid sequences determined were definitely found in the complete amino acid sequence deduced from the nucleotide sequence (Fig. 5, underlined). A common type 1 copper-binding motif [Cys79-(X)<sub>n</sub>-His82-(X)<sub>n</sub>-Met87 in the mature HdBCP sequence] is clearly found in the deduced amino acid sequence of mature HdBCP. The HdBCP sequence shows significant similarities with those of PAz's from various methylotrophic and denitrifying bacteria, *Paracoccus pantotrophus* (Pp) (50% identity), Af (41%), Ac (43%) and Me (45%). A characteristic region containing two short helices region at the C-termini of all PAz's, is also observed in the C-terminus of HdBCP (Lys95 to Gln124). Furthermore, according to the analysis using the newly designed protein signatures for the different BCPs (48), the specific motif [K]-[C]-[T/A]-[P]-[H]-x-[G/A/M]-[M]-[G/S]-[M] for PAz is completely conserved in the HdBCP sequence. From these results, we identified HdBCP with PAz. The amino acid sequence alignment of Hd PAz (HdPAz) is shown with those of PAz's from the denitrifying bacteria in Fig. 6. The possible copper ligands are His41, Cys79, His82 and Met87.

In conclusion, we have found and characterized a unique BCP from Hd. The spectroscopic character of HdBCP shows typical 'perturbed' type 1 copper features in the electronic absorption, CD and EPR spectra. The stopped-flow kinetics of ET between HdBCP and Cyt *c*<sub>L</sub> indicates that not only Cyt *c*<sub>550</sub> but also HdBCP function as an excellent electron acceptor for Cyt *c*<sub>L</sub> in the periplasmic space. Moreover, the nitrite-reducing activity of HdNIR has been also assayed directly by using reduced HdBCP as an electron donor. The catalytic turnover (*k*<sub>cat</sub>) is estimated to be 24 s<sup>-1</sup> in 20 mM phosphate buffer (pH 6.5) containing 100 μM HdBCP. This result suggests that HdBCP also serves as an electron donor for NIR. This bacterium perhaps

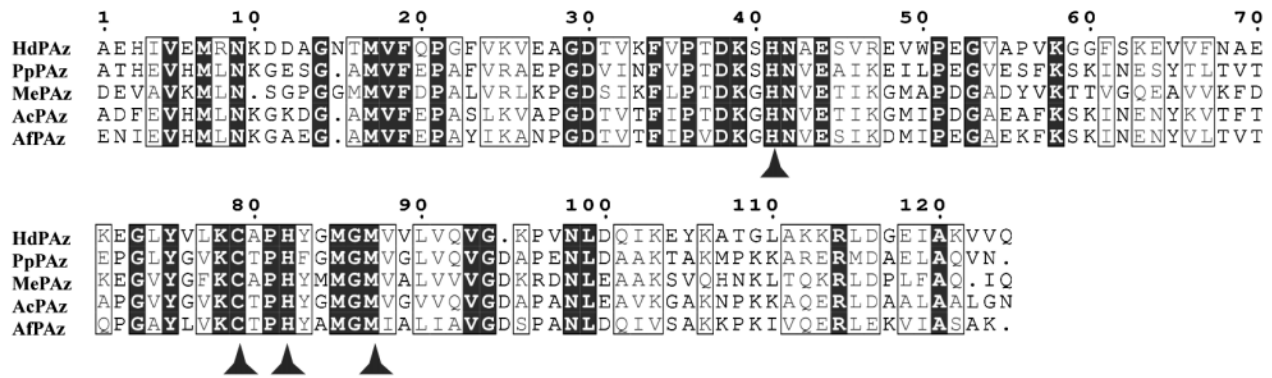


Fig. 6. Alignment of the deduced amino acid sequences of HdPAz and four PAz's. Their amino acid sequences were aligned using the ESPript online site (<http://espript.ibcp.fr/ESPript/ESPript/>). A similarity of the amino acid sequences of HdPAz with those of four PAz's was computed with the default

parameter set (Similarity Groval Score, 0.7 and Similarity Matrix, Risler). Conserved residues are in the boxes, identical residues among five sequences are indicated by white letters on black background and grey letters indicates similar residues. The Cu ligands are marked with black triangles.

maintains the important ET processes from 'methanol oxidation' initialized by MDH to the 'nitrate respiration (denitrification)' even under the conditions of environmental stress such as poor Fe environment. Similar observations by the genetic approach have been reported on a methylotrophic denitrifying bacterium, *P. denitrificans* (49). Cloning and sequence analysis clearly shows that HdBCP is a kind of PAz. In the present study, the stopped-flow kinetics of the ET process between PAz and Cyt  $c_L$  was first observed in the methylotrophic denitrifying bacteria.

We thank Prof K. Tanizawa and Dr T. Okajima (The Institute of Scientific and Industrial Research, Osaka University) for assistance in using a Model 477A protein sequencer. This research was supported by the 21st Century Center of Excellence Program 'Creation of Integrated EcoChemistry' of Osaka University (to D. H.) from Ministry of Education, Culture, Sport, Science and Technology, Japan.

#### REFERENCES

- Aida, T. and Nomoto, K. (1988) Nitrate removal from a sewage by supplementation of methanol using a submerged soil column, and changes in the population of methanol-utilizing denitrifiers in the column soil. *Jpn. J. Soil Sci. Plant Nutr.* **59**, 464–470
- Sperl, G.T. and Hoare, D.S. (1971) Denitrification with methanol: a selective enrichment for *Hyphomicrobium* species. *J. Bacteriol.* **108**, 733–736
- Anthony, C. (2004) The quinoprotein dehydrogenases for methanol and glucose. *Arch. Biochem. Biophys.* **428**, 2–9
- Anthony, C. and Williams, P. (2003) The structure and mechanism of methanol dehydrogenase. *Biochim. Biophys. Acta* **1647**, 18–23
- Anthony, C. (1996) Quinoprotein-catalyzed reactions. *Biochem. J.* **320**, 697–711
- Anthony, C. (1993) Methanol dehydrogenase in gram-negative bacteria in. *Principles and Applications of Quinoproteins* (Davidson, V. L., ed.) pp. 17–45 Marcel Dekker, Inc., New York
- Anthony, C. (1993) The role of quinoproteins in bacterial energy transduction in. *Principles and Applications of Quinoproteins* (Davidson, V. L., ed.) pp. 223–244 Marcel Dekker, Inc., New York
- Nojiri, M., Hira, D., Yamaguchi, K., Okajima, T., Tanizawa, K., and Suzuki, S. (2006) Crystal structures of cytochrome  $c_L$  and methanol dehydrogenase from *Hyphomicrobium denitrificans*: structural and mechanistic insights into interactions between the two proteins. *Biochemistry* **45**, 3481–3492
- Frank, J. and Duine, J.A. (1990) Cytochrome  $c_L$  and cytochrome  $c_H$  from *Hyphomicrobium* X. *Methods Enzymol.* **188**, 303–308
- Day, D.J. and Anthony, C. (1990) Soluble cytochromes  $c$  of methanol-utilizing bacteria. *Methods Enzymol.* **188**, 298–303
- Read, J., Gill, R., Dales, S.L., Cooper, J.B., Wood, S.P., and Anthony, C. (1999) The molecular structure of an unusual cytochrome  $c_2$  determined at 2.0 Å; the cytochrome  $c_H$  from *Methylobacterium extorquens*. *Protein Sci.* **8**, 1232–1240
- Deligeer, F., Kataoka, K., Yamaguchi, K., Kobayashi, K., Tagawa, S., and Suzuki, S. (2002) Spectroscopic and functional characterization of Cu-containing nitrite reductase from *Hyphomicrobium denitrificans* A3151. *J. Inorg. Biochem.* **91**, 132–138
- Yamaguchi, K., Kataoka, K., Kobayashi, M., Itoh, K., Fukui, A., and Suzuki, S. (2004) Characterization of two type 1 Cu sites of *Hyphomicrobium denitrificans* nitrite reductase: a new class of copper-containing nitrite reductase. *Biochemistry* **43**, 14180–14188
- Yamaguchi, K., Kawamura, A., Ogawa, H., and Suzuki, S. (2003) Characterization of nitrous oxide reductase from a methylotrophic denitrifying bacterium, *Hyphomicrobium denitrificans*. *J. Biochem.* **134**, 853–858
- Nojiri, M., Xie, Y., Inoue, T., Yamamoto, T., Matsumura, H., Kataoka, K., Deligeer, F., Yamaguchi, K., Kai, Y., and Suzuki, S. (2007) Structure and function of a hexameric copper-containing nitrite reductase. *Proc. Natl. Acad. Sci. USA* **104**, 4315–4320
- Tobari, J. (1984) Blue copper proteins in electron transport in methylotrophic bacteria in. *Microbial growth on C1 compounds* (Crawford, R.L. and Hanson, R.S., eds.) pp. 106–112 American Society for Microbiology, Washington
- Ambler, R.P. and Tobari, J. (1985) The primary structures of Pseudomonas AM1 amicyanin and pseudoazurin. *Biochem. J.* **232**, 451–457
- Tobari, J. and Harada, Y. (1981) Amicyanin: an electron acceptor of methylamine dehydrogenase. *Biochem. Biophys. Res. Commun.* **101**, 502–508

19. Husain, M. and Davidson, V.L. (1985) An inducible periplasmic blue copper protein from *Paracoccus denitrificans*. *J. Biol. Chem.* **260**, 14626–14629
20. Husain, M., Davidson, V.L., and Smith, A.J. (1986) Properties of *Paracoccus denitrificans* amicyanin. *Biochemistry* **25**, 2431–2436
21. Gray, K.A., Davidson, V.L., and Knaff, D.B. (1988) Complex formation between methylamine dehydrogenase and amicyanin from *Paracoccus denitrificans*. *J. Biol. Chem.* **263**, 13987–13990
22. Chen, L., Durley, R., Poliks, B.J., Hamada, K., Chen, Z., Mathews, F.S., Davidson, V.L., Satow, Y., Huizinga, E., Vellieux, F.M.D., and Hol, W.G.J. (1992) Crystal structure of an electron-transfer complex between methylamine dehydrogenase and amicyanin. *Biochemistry* **31**, 4959–4964
23. Cunane, L.M., Chen, Z.W., Durley, R.C.E., and Mathews, F.S. (1996) X-ray structure of the cupredoxin amicyanin, from *Paracoccus denitrificans*, refined at 1.31 Å resolution. *Acta Crystallogr.* **D52**, 676–686
24. Ambler, R.P. and Tobari, J. (1989) Two distinct azurins function in the electron-transport chain of the obligate methylotroph *Methylobacterium* sp. *Biochem. J.* **261**, 495–499
25. Taguchi, K., Kudo, T., and Tobari, J. (1998) Cloning and characterization of the azurin iso-1 gene, concerned with the electron transport chain involved in methylamine/methanol oxidation in the obligate methylotroph *Methylobacterium* sp. strain J. *Biosci. Biotechnol. Biochem.* **62**, 870–874
26. Yamaguchi, K., Deligeer, , Nakamura, N., Shidara, S., Iwasaki, H., and Suzuki, S. (1995) Isolation and characterization of two distinct azurins from *Alcaligenes xylosoxidans* subsp. *xylosoxidans* NCIB11015 or GIFU1051. *Chem. Lett.*, **1995**, 353–354
27. Dodd, F.E., Hasnain, S.S., Hunter, W.N., Abraham, Z.H.L., Debenham, M., Kanler, H., Eldridge, M., Eady, R.R., Ambler, R.P., and Smith, B.E. (1995) Evidence for two distinct azurins in *Alcaligenes xylosoxidans* (NCIMB 11015): Potential electron donors to nitrite reductase. *Biochemistry* **34**, 10180–10186
28. Dodd, F.E., Hasnain, S.S., Abraham, Z.H.L., Eady, R.R., and Smith, B.E. (1995) Structure of a new azurin from the denitrifying bacterium *Alcaligenes xylosoxidans* at high resolution. *Acta Crystallogr.* **D51**, 1052–1064
29. Li, C., Inoue, T., Gotowda, M., Suzuki, S., Yamaguchi, K., Kataoka, K., and Kai, Y. (1998) Structure of azurin I from the denitrifying bacterium *Alcaligenes xylosoxidans* NCIMB 11015 at 2.45 Å resolution. *Acta Crystallogr.* **D54**, 347–354
30. Inoue, T., Kai, Y., Harada, S., Kasai, N., Ohshiro, Y., Suzuki, S., Kohzuma, T., and Tobari, J. (1994) Refined crystal structure of pseudoazurin from *Methylobacterium extorquens* AM1 at 1.5 Å resolution. *Acta Crystallogr.* **D50**, 317–328
31. Kohzuma, T., Dennison, C., McFarlane, W., Nakashima, S., Kitagawa, T., Inoue, T., Kai, Y., Nishio, N., Shidara, S., Suzuki, S., and Sykes, A.G. (1995) Spectroscopic and electrochemical studies on active-site transitions of the type 1 copper protein pseudoazurin from *Achromobacter cycloclastes*. *J. Biol. Chem.* **270**, 25733–25738
32. Suzuki, S., Nakamura, N., Yamaguchi, K., Kataoka, K., Inoue, T., Nshio, N., Kai, Y., and Tobari, J. (1999) Spectroscopic and electrochemical properties of two azurins (Az-iso1 and Az-iso2) from the obligate methylotroph *Methyromonas* sp. strain J and the structure of novel Az-iso2. *J. Biol. Inorg. Chem.* **4**, 749–758
33. Kohzuma, T., Takase, S., Shidara, S., and Suzuki, S. (1993) Electrochemical properties of copper proteins, pseudoazurin and nitrite reductase from *Achromobacter cycloclastes* IAM 1013. *Chem. Lett.*, **1993**, 149–152
34. Kukimoto, M., Nishiyama, M., Ohnuki, T., Turley, S., Adman, E.T., and Horinouchi, S. (1995) Identification of interaction site of pseudoazurin with its redox partner, copper-containing nitrite reductase from *Alcaligenes faecalis* S-6. *Protein Eng.* **8**, 153–158
35. Kukimoto, M., Nishiyama, M., Tanokura, M., Adman, E.T., and Horinouchi, S. (1996) Studies on protein-protein interaction between copper-containing nitrite reductase and pseudoazurin from *Alcaligenes faecalis* S-6. *J. Biol. Chem.* **271**, 13680–13689
36. Suzuki, S., Kataoka, K., Yamaguchi, K., Inoue, T., and Kai, Y. (1999) Structure-function relationships of copper-containing nitrite reductases. *Coordin. Chem. Rev.* **190–192**, 245–265
37. Zannoni, D. (1989) The respiratory chains of pathogenic pseudomonas. *Biochim. Biophys. Acta* **975**, 299–316
38. Zumft, W.G., Gotzmann, D.J., and Kroneck, P.M. (1987) Type 1, blue copper proteins constitute a respiratory nitrite-reducing system in *Pseudomonas aureofaciens*. *Eur. J. Biochem.* **168**, 301–307
39. Vijgenboom, E., Busch, J.E., and Canters, G.W. (1997) *In vivo* studies disprove an obligatory role of azurin in denitrification in *Pseudomonas aeruginosa* and show that *azu* expression is under control of RpoS and ANR. *Microbiology* **143**, 2853–2863
40. Sakurai, T., Okamoto, H., Kawahara, K., and Nakahara, A. (1982) Some properties of a blue copper protein 'plantacyanin' from cucumber peel. *FEBS Lett.* **147**, 220–224
41. LaCroix, L.B., Randall, D.W., Nersissian, A.M., Hoitink, C.W.G., Canters, W.G., Valentine, J.S., and Solomon, E.I. (1998) Spectroscopic and geometric variations in perturbed blue copper centers: electronic structures of stellacyanin and cucumber basic protein. *J. Am. Chem. Soc.* **120**, 9621–9631
42. Solomon, E.I., Szilagyi, R.K., George, S.D., and Basumallick, L. (2004) Electronic structures of metal sites in proteins and models: contributions to function in blue copper proteins. *Chem. Rev.* **104**, 419–458
43. Solomon, E.I., Hare, J.W., Dooley, D.M., Dawson, J.H., Stephens, P.J., and Gray, H.B. (1980) Spectroscopic studies of stellacyanin, plastocyanin, and azurin: electronic structure of the blue copper sites. *J. Am. Chem. Soc.* **102**, 168–178
44. Suzuki, S., Sakurai, T., Shidara, S., and Iwasaki, H. (1989) Spectroscopic characterization of cobalt(II)-substituted *Achromobacter* pseudoazurin: similarity of the metal center in Co(II)-pseudoazurin to those in Co(II)-plastocyanin and Co(II)-plantacyanin. *Inorg. Chem.* **28**, 802–804
45. Petratos, K., Banner, D.W., Beppu, T., Wilson, K.S., and Tsernoglou, D. (1987) The crystal structure of pseudoazurin from *Alcaligenes faecalis* S-6 determined at 2.9 Å resolution. *FEBS Lett.* **218**, 209–214
46. Petratos, K., Danter, Z., and Wilson, K.S. (1988) Refinement of the structure of pseudoazurin from *Alcaligenes faecalis* S-6 at 1.55 Å resolution. *Acta Crystallogr.* **B44**, 628–636
47. Guss, J.M., Merritt, E.A., Phizackerley, R.P., Hedman, B., Murata, M., Hodgson, K.O., and Freeman, H.C. (1988) Phase determination by multiple-wavelength x-ray diffraction: crystal structure and a basic 'blue' copper protein from cucumbers. *Science* **241**, 806–811
48. Giri, A.V., Anishetty, S., and Gautam, P. (2004) Functionally specified protein signatures distinctive for each of the different blue copper proteins. *BMC Bioinform* **5**, 127–135
49. Ferguson, S.J. (1998) The *Paracoccus denitrificans* electron transport system: aspects of organisation, structures and biogenesis in. in *Biological Electron Transfer Chains: Genetics, Composition and Mode of Operation* (Canters, G.W. and Vijgenboom, E., eds.) pp. 77–88 Kluwer Academic Publishers, The Netherlands